PLANETARY INVESTIGATION UTILIZING AN IMAGING SPECTROMETER SYSTEM BASED UPON CHARGE INJECTION TECHNOLOGY

R. B. Wattson, P. Harvey, and R. Swift
American Science & Engineering, Inc.
Cambridge, Massachusetts

An intrinsic silicon charge injection device (CID) television sensor array has been used in conjunction with a $CaMoO_4$ co-linear tunable acousto-optic filter, Harvard's 61-inch reflector, a sophisticated computer system, and a digital color TV scan converter/computer to produce near-IR images of Saturn and Jupiter with 10-Å spectral resolution and ~3-inch spatial resolution.

The CID camera has successfully obtained digitized 100 × 100 array images with 5 minutes of exposure time, slow-scanned readout to a computer (300 ms and digitized to 12-bit accuracy), and has produced this data at near dry ice temperature and in conjunction with other state-of-the-art technology instrumentation. Details of the equipment setup, innovations, problems, experience, data and final equipment performance limits are given, so that those people who plan to utilize solid-state TV sensor arrays will be able to judge, at least in part, which technology, CCD or CID, they should choose. Twelve spectral images of Saturn are shown, 40 Å apart (centered at 8500 Å), which will illustrate the type of data now obtainable with present CID technology. It is our belief that the

data represents the first instance of truly three-dimensional astronomical data that has been obtained.

I. INTRODUCTION

Figures 1a and b are images of Saturn having ~3-inch spatial resolution. Each image represents a 10-Å spectral bandpass in the near infrared, and required about 5 minutes of exposure due to the narrow bandpass. The twelve spectral images of Figure 1a are generally 40 Å apart, as indicated by the central wavelengths shown below each image (the first image should indicate 9400 Å). Although some corrections for background and noise have been applied, it is not valid to compare the overall intensities of different spectral images. However, the variation of ball-to-ring intensity ratios for the different images is significant. The absence of Saturn's ball at 8900 Å and 8860 Å and the depression of the ball relative to the rings near 8700 Å is clearly evident. Note also the bright equatorial bulge in the planet seen at 8780 Å. This may be caused by higher clouds and hence less methane absorption near Saturn's equatorial region. It is interesting to compare the relative ball-to-ring intensities vs. wavelength with the reflectivity spectrum of Jupiter shown in Figure 2, from Pilcher et al. (Ref. 1). The dots, indicating the wavelengths of the Saturn images of Figure 1a, encompass a methane double absorption feature with a strong dip at 8900 Å and a more moderate dip at 8700 Å. The spectral resolution is 10 Å in both Figures 1 and 2.

Figure 1b shows both a spectral image of Saturn (8660 Å) and a spatial intensity plot for a line through the planet. The location of the line is indicated by tick marks on the image. Note the good S/N (~20:1) of the plot. The intensity scans for Saturn's ball are essentially limb-darkening curves. These curves are being analyzed by fitting to Minnaert functions for various wavelengths.

These and other spectral images of Saturn, ranging from 7200 Å to 10, 600 Å (i. e., essentially the range covered by Figure 2), and a similar set of images of Jupiter, were obtained from data taken at Harvard's 61-inch reflector during December 1974 and early January 1975. They were acquired by the use of a new type of instrumentation, an imaging spectrometer, which is the subject of this paper.

II. DESCRIPTION OF INSTRUMENTATION

Figure 3a shows a schematic of the imaging spectrometer. Figure 3b is a picture of the instrument, which is about 2 feet long. It consists of two principal parts: a tunable acousto-optic filter (TOF) (Ref. 2) and a charge injection device (CID) camera (Ref. 3). The TOF is similar in throughput and transmission characteristics to an interference filter of comparable resolution, except that it is electronically tunable over a 2:1 wavelength range. The TOF utilizes a pair of crossed calcite Glan-Thompson polarizers, between which is placed a bi-refringent $CaMoO_4$ crystal. Acoustic waves, produced by a voltage-controlled oscillator and piezo-electric transducer, are propagated axially through the bi-refringent crystal and absorbed at the opposite end. Polarized light transmitted through the crystal in a direction co-linear with the acoustic waves interacts with the acoustic field in such a way that only a narrow range of wavelengths, related to the acoustic frequency, is scattered into the other polarization state and is thus transmitted by the output polarizer. The filter's bandpass is basically determined by the same characteristic that determines the bandpass of a diffraction grating monochromator: the number of grating rulings; correspondingly, in the TOF, the number of acoustic waves in the crystal determines its resolution. Computer control of the rf driving frequency is possible.

The other optics of the imaging spectrometer include relay lenses to transmit the primary telescope image through the TOF and onto the CID chip; a beam splitter, reticle and eyepiece which are used for manual guidance of the telescope during exposure; and a cylindrical lens to correct for the astigmatism produced by the TOF's bi-refringence.

The CID camera is basically an intrinsic silicon 100 × 100 sensor array, wherein each sensor is ~0.1 mm square. Each sensor has a quantum efficiency of ~50% at 9000 Å and, at -40° C, shows only moderate integrated dark current after 5 minutes exposure time. The CID, like the CCD cameras, employs a passive solid-state digital readout mode instead of either the active digital readout mode of photodiode arrays such as Reticon arrays or an electron-beam readout mode as exemplified by the silicon target vidicon cameras. Highly monochromatic radiation, such as is used in this system, may produce interference effects in a vidicon system. No such effect has been observed with the present TOF/CID system having a 10-Å bandpass.

The charge injection device readout employs the injection of a particular sensor's charge into the silicon substrate via the voltage change across a row/column addressed capacitor at the sensor site. Other sensor sites along the particular row or column only have their charges shifted. With this technique, random sensor interrogation could be achieved if desired. Charge-coupled technology, on the other hand, requires many transfers via capacitor plates to translate the entire charge pattern resulting from the image to a storage area for line-by-line readout, thereby requiring extremely high transfer efficiency.

The GE CID camera, which was originally designed for standard TV frame rates, had a readout rate fixed at about 300 kHz continuous, and used a triggered analog sweep system, so that after injection significant amounts of signal remained uncollected. At AS&E, the camera was modified by installing interrupt circuitry to hold the digital camera sweep at the beginning of the first field until triggered by a computer, one sweep at a time. The injection time was increased and the internal readout clock rate decreased; a digital monitor sweep system was constructed which would track the camera sweep regardless of rate. The output signals were amplified, DC restored, digitized, and sent via line drivers to the computer.

The CID chip was found to saturate on dark current in about 3 seconds at room temperature. Since the expected signals would require integration for much longer periods of time, it was necessary to cool the CID chip to reduce both the dark current and its associated shot noise. The characteristics of reverse-biased Si are such that the dark current can be expected to decrease by approximately a factor of two for every 10° C cooling. Thus, at the temperature of dry ice, or some 100° C below room temperature, we would expect to be able to integrate for about half an hour without dark current saturation.

In order to achieve such cooling, the CID chip was removed from its socket in the camera body and mounted on an ~1-inch extender, so that it could be located within a cooled, insulated enclosure. The extender was fabricated from a spare header and socket, provided by GE, sandwiched around a block of lucite. The interconnections were made by means of fine (#30) wire to minimize heat conduction. The enclosure is (literally) a peanut can, lined with polystyrene foam and provided with a double-paned window, evacuated between the panes to provide a thermal barrier that does not frost. The assembly was

attached to the camera body at the normal lens location. The enclosure was continuously purged with dry nitrogen gas to prevent fogging.

Cooling was done by thermally coupling the CID to a brass heat sink, through which cold alcohol was pumped. Anhydrous, denatured alcohol and 1/4-inch tubing were used to prevent the fluid viscosity from restricting the flow. Several coils of copper tubing immersed in a dry ice/alcohol slurry served as a heat exchanger through which the coolant was circulated. The slurry temperature was about -55° C. This operating temperature for the CID chip is consistent with dark current saturation after ~20 minutes. Dark current buildup was hardly detectable after 5 minutes of integration time.

Experience with the CID camera, operated under extremely cold (-15° C) and also under humid ambient conditions, showed that modification and refurbishment of both the prototype electronics and the CID sensor array were needed. With strong cooperation from GE, both were done. Because of the longer injection times and the small capacitances involved in the readout circuitry, the printed circuit board became a significant leakage path due to condensation or humidity in the telescope environment. The problem was overcome by thoroughly cleaning and drying the board and spraying it with Krylon clear plastic. Hermetic sealing of the CID chip, to overcome moisture contamination problems, was done at GE. Very little difficulty with the CID camera has been experienced since these changes were made. The data and accumulated experience indicate that the expertise now exists to allow reliable field use of CID cameras, at least for ground-based observational purposes.

Frame integration time was determined by the operator, who had control of the system via an alphanumeric computer terminal. When the program determines that an exposure is complete, the computer initiates the CID readout mode. The 10^4-word, 12-bit readout of the CID camera was read directly into the 32K core of a NOVA 1200 via the data channel. The data were then stored on digital tape and, for random access to spectral image frames, stored also on magnetic discs.

One of the main design philosophies of the system was real-time display of the data, allowing the operator to exercise his judgment to repeat exposures and/or modify or improve the data acquisition parameters based upon the observed results. Hence, a display computer/scan converter and a color TV

monitor were used to immediately view the images as they were acquired. The use of color can enhance the observer's ability to discriminate against improper data. Some degree of processing can also be accomplished before display. Various other display modes such as alphanumeric information and plots are available at the operator's command. The images shown in Figure 1 were produced directly via this display system.

Finally, the entire computer support facility (shown in Figure 4) is portable. It is sufficiently small and reliable to be transported and operated anywhere, having already been used at several sites without major difficulty.

III. CONCLUSIONS

The data displayed here represents only the first very preliminary and relatively crude data obtained by an imaging spectrometer system designed for astronomical observations. Improvements of factors of 3 or more in instrumental sensitivity, spatial resolution and demonstrable spectral resolution can be made by improved CID preamp design, reduced residual bi-refringent aberrations and extended observation time. Careful photometric calibration and spatial, spectral and vignetting corrections, combined with use of observation sites more suited to planetary observations (i.e., observation sites where relatively long exposures can be accomplished with 1-inch or better "seeing" and guiding characteristics), will provide very useful new planetary results. Extension of the spectral response to the 5-μm region is possible by the use of InSb CIDs and TeO_2 TOFs. Observation sites located above the earth's atmosphere would eliminate atmospheric interference in that spectral region, and would extend the spatial resolution to the diffraction limit. Finally, sophisticated radiative transfer algorithms employing anisotropic, inhomogeneous atmospheric modeling will enable one to construct, via planetary atmospheric molecular absorption features, truly three-dimensional pressure, temperature, constituent and aerosol maps of planetary atmospheres. Such pixel-by-pixel "sounding" maps can be made with the existing equipment for CH_4 and NH_3 on Jupiter and Saturn, CO_2 on Venus and, in fact, the present spectral resolution may even allow 1-inch maps separating the J-manifolds of the R-branch $3\nu_3$, CH_4 band! Hence, one could say that the technique described above represents the beginning of true 3-D planetary astronomy.

ACKNOWLEDGEMENTS

Much appreciation is extended to the directors and staff of the Harvard Observatory for their strong cooperation in the observational program. The authors would also like to thank Dr. Edwin Frederick and Dr. Saul Rappaport as co-observators, and Richard Cabral and Douglas Hill for their very helpful engineering in this effort.

REFERENCES

1. C. B. Pilcher, R. G. Prinn, and T. B. McCord, J. Atmos. Sci., 30, 302 (1973).

2. S. E. Harris, S. T. K. Nieh, and D. K. Winslow, "Electronically Tunable Acousto-Optic Filter," Applied Physics Letters, 15, 325 (1969).

3. G. J. Michon and H. K. Burke, "Charge Injection Imaging," IEEE International Solid-State Circuits Conference Digest, 138-139 (1973).

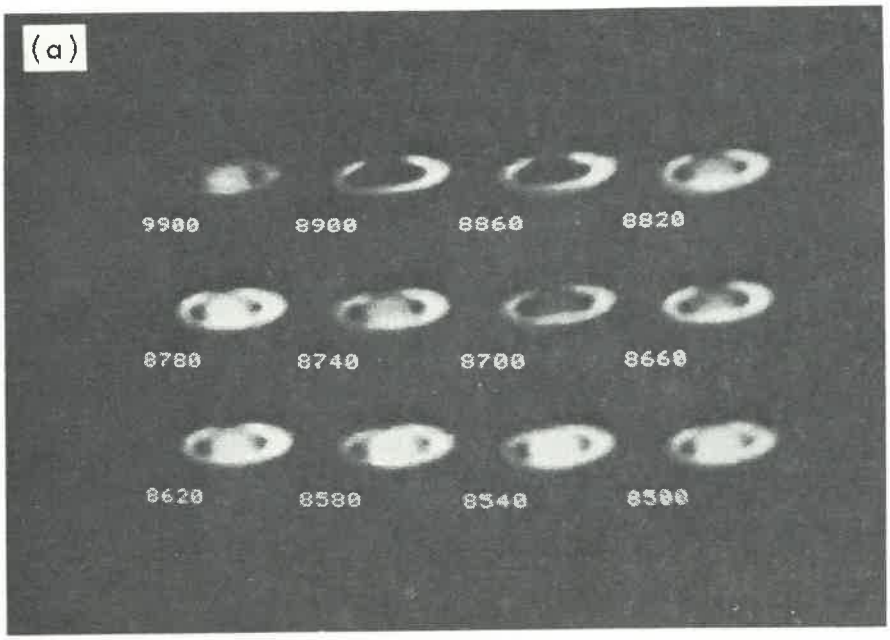

Figure 1a. Twelve images of Saturn at wavelengths ranging from 8500 to 9400 Å

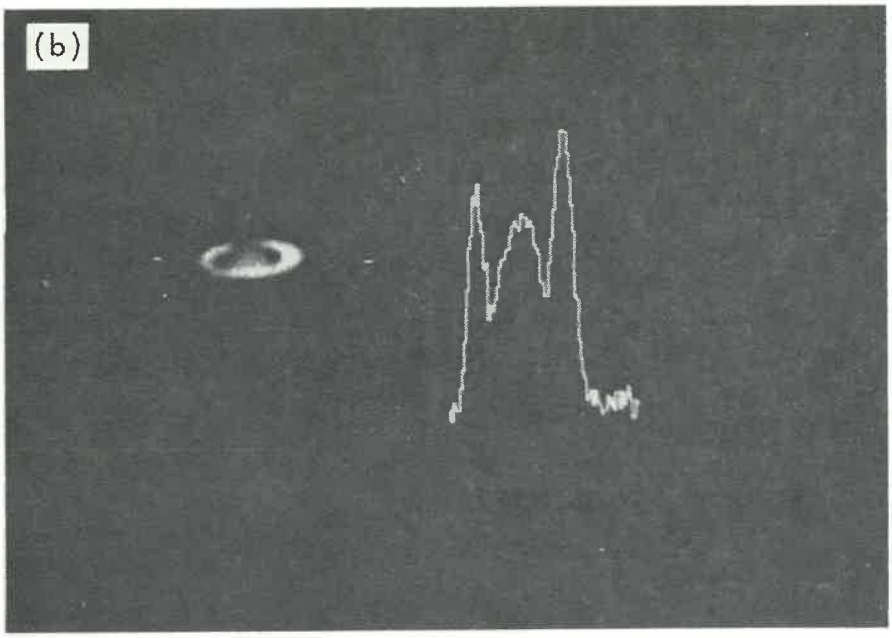

Figure 1b. Spectral image and cross-sectional intensity plot of Saturn at 8660 Å

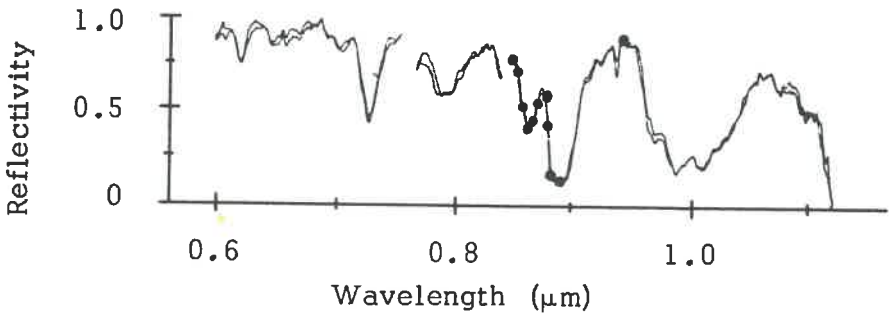

Figure 2. Absolute reflectivities of Jupiter (Ref. 1)

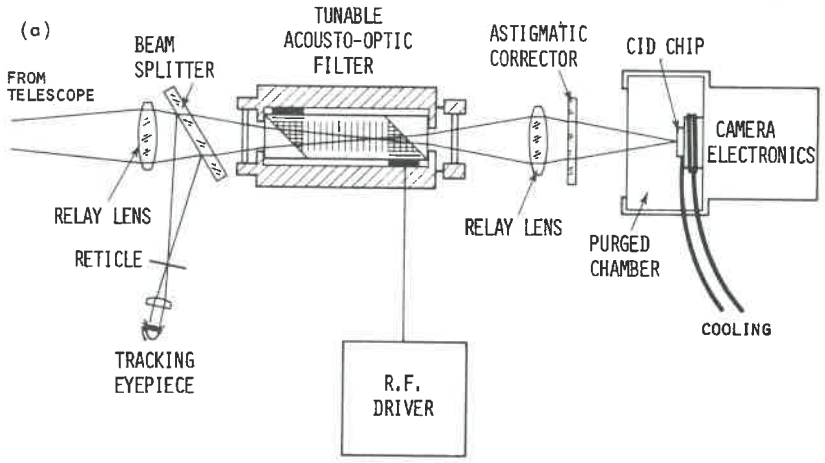

Figure 3a. Schematic diagram showing principal components of the imaging spectrometer

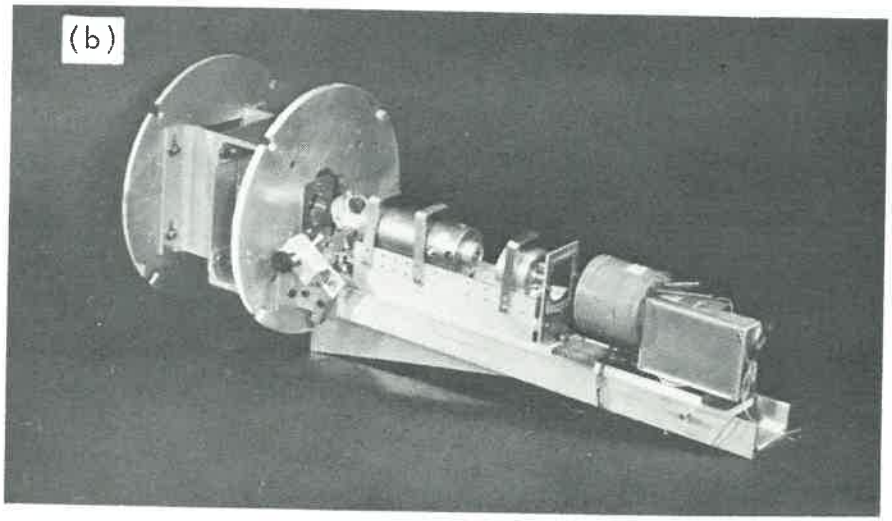

Figure 3b. Photograph of the imaging spectrometer

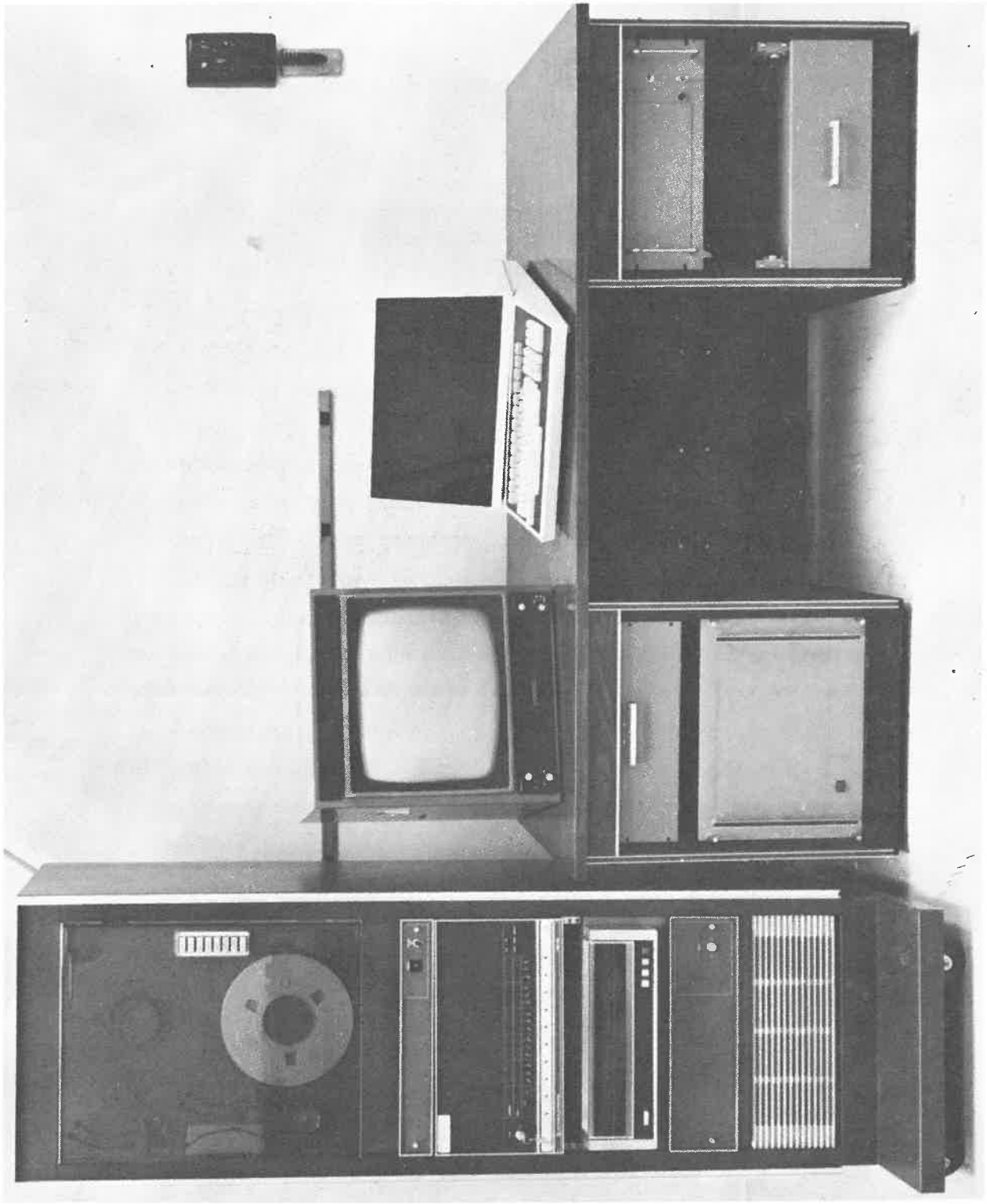

Figure 4. Processing and display facility